## PAPER

Check for updates

# Tuning the efficiency of molecular probes *via* quinone methide-based *in situ* labeling

Zachary Rabinowitz, [ID] †[a] Seyedehalaleh Anvar, [ID] †[a] Jun Liu,†[ab] Zixin Chen, [ID][a]
Yuzhao Zhang, [ID][a] Chao Cui,[a] Ashton Sigler [ID][b] and Lina Cui [ID] ⋆[ab]

Imaging the activities of hydrolases using molecular imaging probes can reveal underlying molecular mechanisms in the context of cells to organisms and their correlation with different pathological conditions can be used in diagnosis. Due to the nature of hydrolases, substrate-based probes can take advantage of their catalytic cycles to free reporter moieties that can generate amplified signal. This is less ideal in the context of cell- or organism-based detection, as the reporter moiety can easily diffuse away from the target site upon activation. Therefore, spatial resolution is a key factor for probe sensitivity. One strategy to improve the spatial resolution is to form a covalent linkage between the reporter moiety and intracellular proteins upon probe activation by the enzyme *via* a reactive intermediate. In this work, we tuned the reactivity of the quinone methide intermediate by synthesizing fluorescent probes containing different modifications to the phenol linker for β-galactosidase activation. The labeling efficacy of these probes was evaluated using fluorescence gel electrophoresis, flow cytometry, and fluorescence cell imaging. This study provides insights into the further development of hydrolase-targeting probes for cell- or organism-based imaging with enhanced efficiency *via in situ* labeling.

## Introduction

Molecular imaging probes are important tools to interrogate biological functions, both spatially and temporally, in living cells and organisms.[1] Probes can be constructed to detect a myriad of different biological molecules including hydrolases. Hydrolases, enzymes that catalyze hydrolysis of their substrates, are important biomolecules that are involved in a wide range of biological functions. Like other biomolecules, their activities can become enhanced or diminished in diseased states, compared to healthy states. Thus, detecting or imaging the activities of hydrolases can reveal underlying molecular mechanisms in the context of cells-to-organisms, and their correlation with different pathological conditions can be used in diagnosis.[2] Due to the nature of hydrolases, substrate-based probes can be activated in their catalytic cycles. Subsequently, hydrolysis of the substrate frees reporter moieties that provide either positive or negative signal output. Substrate-based probes have been widely used to assess enzyme activities in various contexts *in vitro* or *in vivo*, taking advantage of their catalytic cycles for amplified signals.[3]

A major limitation of most substrate-based small molecule imaging probes is that they can easily diffuse away from the site of activation, resulting in poor sensitivity and low signal-to-background ratios.[4] For test-tube type bulk detection, spatial resolution is not a measure of importance. However, for cell- or organism-based detection or imaging, spatial resolution is a key factor for probe sensitivity that influences signal-to-background ratios.[5] Various strategies have been developed to improve spatial resolution.[6–8] For example, small molecule probes can be activated by the target enzyme, and due to the change in hydrophobicity before and after enzyme activation, they can self-assemble into nanometer-sized particles or aggregates and retain at the site of activation.[9–16] Alternatively, using previously developed strategies for targeted covalent inhibitors,[17,18] a covalent bond between the probe and an intracellular, nucleophilic protein can be formed *via* the formation of an electrophilic moiety generated upon activation of the probe.[6,19–22]

Quinone methides (QMs) are a reactive, electrophilic species that can be generated *in situ* from a protected phenol precursor bearing a leaving group on the methyl group at either the *para*- or *ortho*-position.[23–27] Once formed, QMs are susceptible to nucleophilic attack. Under physiological conditions, QMs can be formed *via* removal of a "blocking" group, resulting in unmasking of the phenolic oxygen and loss of a leaving group. Enabling bioorthogonal QM chemistry has found numerous applications including developing activity-based probes for various enzymes (*e.g.*, phosphatase,[28] glycosidases,[29–38] tyrosine

*a Department of Medicinal Chemistry, College of Pharmacy, University of Florida, Gainesville, FL 32610, USA. E-mail: linacui@cop.ufl.edu*

*b Department of Chemistry and Chemical Biology, University of New Mexico, Albuquerque, NM 87131, USA*

† These authors contributed equally.

phosphatase,[39] steroid sulfatase,[40] and beta-lactamase[41–43]), prodrugs,[44–46] among others.[47–50]

Across these applications, fluorine of either the mono- or difluoromethyl group has been frequently used as the leaving group to form the active quinone methide intermediate *via* spontaneous elimination of a molecule of hydrogen fluoride (HF).[26] However, the application of *in situ* labeling of biological molecules *via* QM chemistry has been dwarfed by the dilemma that the monofluoromethyl group is more reactive, yet the conjugated products are more stable than its difluoromethyl counterpart.[31,41,51] Some molecules containing a monofluoromethyl group suffer from poor stability in aqueous media due to hydrolysis or non-specific reactivity with other nucleophilic molecules before the probe reaches the active site of the target enzyme.[52,53] Depending on the properties of the molecules, some monofluoromethyl group-containing probes are reportedly stable,[42,54] while many others, including several unpublished probes developed in our lab, are susceptible to hydrolysis.[38,52]

Identification of self-immolative linkers with better stability in solution, reactivity profiles, and labeling efficiencies remains an important feat towards applying QM-based probes in various applications. Towards solving this issue, the ethyl carbamate moiety has been used as an alternative leaving group to limit hydrolysis and labeling of non-target nucleophilic molecules.[52,53,55,56] Furthermore, installation of electron-donating- or electron-withdrawing substituents on QMs has been found to modulate the rate of formation and stability of their adducts *in vitro*.[57] However, thorough investigations of altering the leaving group capability and tuning the aromatic ring electronics to enhance the performance of self-immolative phenol linkers are limited.[53] In this paper, we evaluated two different approaches in parallel to provide insights on the design of self-immolative QM-based hydrolase-targeting probes with better stability, reactivity profiles, and labeling efficiencies.

## Results and discussion

### Design and synthesis of QM-based fluorescent probes

Overall, we designed and synthesized probes each containing three moieties: a β-galactoside moiety, a self-immolative phenol linker, and fluorescein (FITC) (Fig. 1). In addition, to enhance the stability of the linkage between the phenol linker and FITC during synthesis, a previously developed *S*-methyl-isothiourea linkage was utilized.[30] The synthesis of these probes was performed as outlined in Scheme S1.

To investigate whether we can improve the performance of QM-based probes, we took two different logical approaches of modifying the self-immolative phenol linker. The first approach is to install a group with better leaving group ability than fluorine. A more stabilized leaving group would theoretically improve the labeling efficiency by facilitating the formation of the QM, which has been shown to be dependent on the type of leaving group.[58] Thus, we designed and synthesized **BG-FITC-OCONHEt** containing an ethyl carbamate leaving group, which is
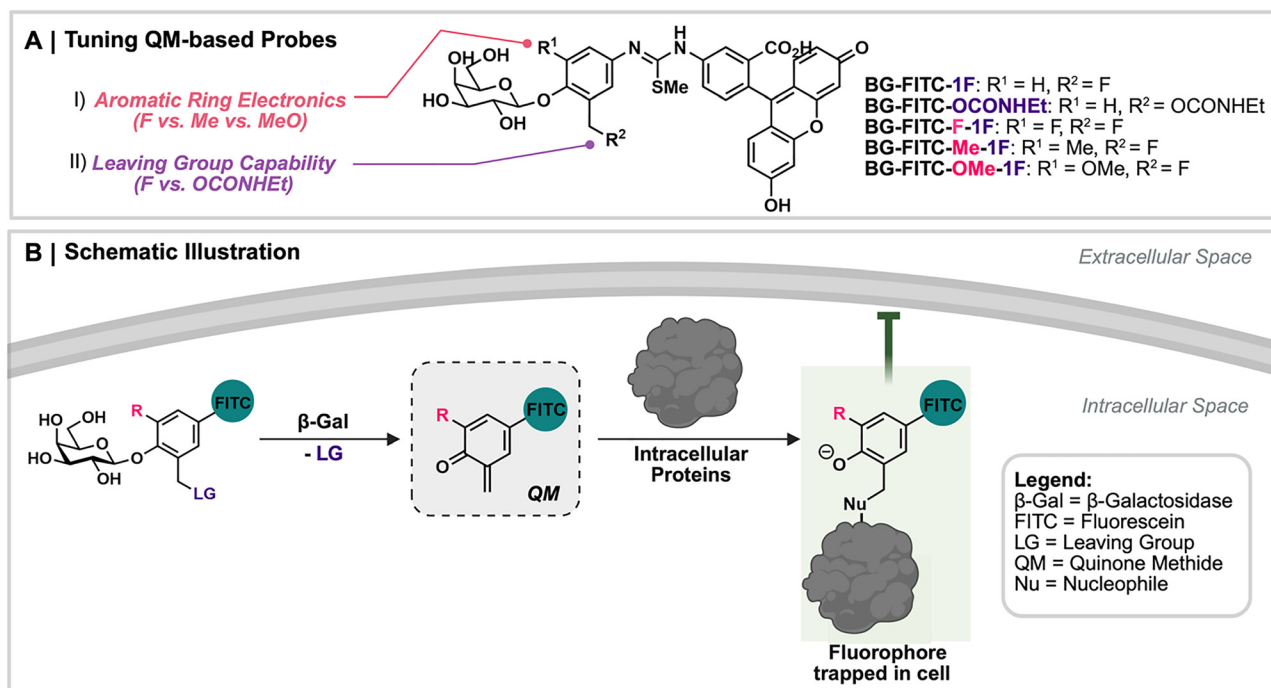


Fig. 1 Tuning the labeling effiency of QM-based Probes. (A) Structures of QM-based probes described herein. Two distinct strategies were explored to tune the self-immolative phenol linker: (I) altering the electronic properties of the aromatic ring through installation of electron-withdrawing groups (*e.g.*, fluorine) or electron-donating groups (*e.g.*, methyl, methoxy) and (II) modulating the leaving group ability to facilitate QM formation. (B) Schematic illustration of the activation mechanism of QM-based *in situ* labeling to enhance cellular retention. Upon activation by β-Gal, the probe generates a highly reactive electrophilic QM intermediate. This intermediate can then react with intracellular nucleophiles such as proteins, forming a covalent bond that traps the fluorophore within the cell and enhances its retention. Created with BioRender.

stabilized through electron delocalization and represents a better leaving group than the small, electronegative fluorine atom (Fig. 1). This rationale is further supported by a prior report that the replacement of fluorine with ethyl carbamate led to a more stable molecule in phosphate-buffered saline (PBS).[52] The second approach is to adjust the electronics of the aromatic linker. The labeling efficiency and stability of the resulting conjugate has been shown to be tunable by installation of substituents on the self-immobilizing phenol linker.[57] To explore how altering the electronics of the aromatic linker affects the labeling efficiency of QM-based probes, electron-donating groups such as methoxy (**BG-FITC-OMe-1F**) and methyl (**BG-FITC-Me-1F**) or electron-withdrawing groups such as fluorine (**BG-FITC-F-1F**) were installed on the aromatic ring in the ortho position to the phenolic oxygen (Fig. 1).

In the presence of β-galactosidase (β-Gal), the β-galactosyl bond is hydrolyzed, allowing the phenol linker to undergo self-immolation to generate the QM in situ upon loss of the leaving group. The QM can then alkylate nearby proteins via their nucleophilic residues. Therefore, we aimed to evaluate and compare the labeling efficiencies (i.e., the amount of FITC-labeled protein) of probes with different modifications in vitro and in living cells to gauge whether we can improve the reactivity profiles and stability of QM-based probes. All probe molecules contained the fluorescent reporter, FITC, in its "on" state, both before and after activation. QM-based probes can also be designed to feature an increase in fluorescence intensity ("turn-on") after removal of the "blocking group" and nucleophilic attack of the QM, making it more sensitive towards analyte detection.[26,38] In this case, without fluorescence change after target activation, our approach provided direct visual comparison of the labeling efficiencies of these molecules both in vitro and in cells.

### Evaluation of labeling efficiency *in vitro*

Prior to evaluating the labeling efficiency of these probes, we first confirmed the concentration of all probe stock solutions and assessed their stability in aqueous solution (Fig. S1 and S2). All probes were stable (at least 95% intact probe) after 4-hours of incubation at 37 °C. Therefore, we carried out the labeling efficiency evaluation of all probes using a 4-hour incubation period. With longer incubation times, **BG-FITC-1F** showed the most degradation, followed by **BG-FITC-F-1F**, **BG-FITC-Me-1F**, and **BG-FITC-OMe-1F**. On the other hand, **BG-FITC-OCONHEt** exhibited superior stability. LC-MS analysis of the byproducts suggested that hydrolysis of both the monofluoromethyl group and *S*-methyl-isothiourea linkage are two mechanisms for probe degradation (data not shown).

To evaluate the labeling efficiency of these probes *in vitro*, we incubated bovine serum albumin (BSA, 1 μg μL$^{-1}$), with 5 μM of each probe with or without *Escherichia coli* β-Gal (0.4 μg μL$^{-1}$) for 4-hours in PBS (pH 7.4) at 37 °C. The resulting mixtures were analyzed by sodium dodecyl sulfate polyacrylamide gel electrophoresis (SDS-PAGE) and the in-gel fluorescence intensities of FITC-labeled BSA were quantified using ImageJ (Fig. 2). As shown in Fig. 2A, in the presence of β-Gal, the probes labeled
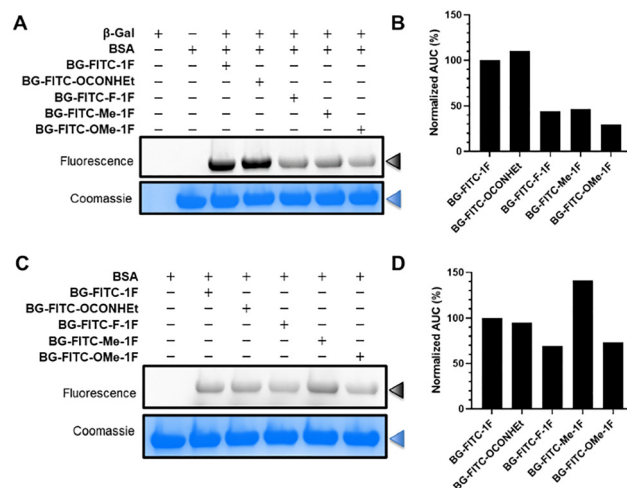


Fig. 2 Evaluation of labeling efficiencies of probes in vitro. SDS-PAGE analysis of BSA (1 μg μL$^{-1}$) after incubation with probes (5 μM) in the (A) presence or (C) absence of β-Gal (0.4 μg μL$^{-1}$) for 4-hours at 37 °C. Images of both inverted fluorescence (top image; FITC channel) and Coomassie blue staining (bottom image; colorimetric channel) of the gel were captured using the Bio-Rad ChemiDoc$^{TM}$ MP Imaging System. Band quantification of FITC-labeled BSA after incubation with probes (5 μM) (B) with or (D) without β-Gal (20 μg) for 4-hours at 37 °C. Inverted fluorescence bands of BSA were quantified using ImageJ (NIH, Bethesda, MD) and normalized to **BG-FITC-1F** for comparison.

BSA with FITC via generation of the QM intermediate, followed by alkylation of the protein. **BG-FITC-OCONHEt** showed a higher labeling efficiency of BSA than **BG-FITC-1F** (Fig. 2B), suggesting that the superior stability in solution as well as the better leaving group ability of the ethyl carbamate group over fluorine of the monofluoromethyl moiety (Fig. S2) may facilitate the formation and yield of the QM intermediate, leading to more labeling of BSA. Surprisingly, tuning the aromatic ring electronics with either electron-donating- (**BG-FITC-Me-1F**, **BG-FITC-OMe-1F**) or electron-withdrawing groups (**BG-FITC-F-1F**) did not show any improvements in the labeling of BSA, compared to **BG-FITC-1F** (Fig. 2B). In the absence of β-Gal, the probe cannot generate the electrophilic, QM intermediate, however, proteins can likely still attack the probe to form a covalent bond via nucleophilic substitution reaction, due to the presence of a leaving group. Moreover, the probes can bind to proteins in a non-covalent fashion, leading to non-specific labeling of BSA and poor specificity. To examine non-QM-mediated labeling of BSA, we incubated 5 μM of each probe with BSA (1 μg μL$^{-1}$) without the addition of *Escherichia coli* β-Gal (Fig. 2C). To our surprise, in-gel fluorescence revealed that **BG-FITC-1F** and **BG-FITC-OCONHEt** exhibited similar non-specific labeling of BSA (Fig. 2D). A previous study observed that molecules containing the less reactive ethyl carbamate leaving group produced less non-specific fluorescence tagging of BSA than fluorine of the monofluoromethyl leaving group.[53] On the other hand, **BG-FITC-F-1F** and **BG-FITC-OMe** showed lower non-specific labeling of BSA than **BG-FITC-1F**, whereas **BG-FITC-Me-1F** exhibited the highest non-specific labeling of BSA (Fig. 2D), suggesting that this probe has more interactions with BSA.

Modification of self-immolative phenol linkers with electron-withdrawing groups (such as ethyl esters) have been shown to result in slow formation of their adducts, however, their adducts are more stable over time.[57] On the contrary, electron-donating groups (such as methyl) gave rise to rapid adduct formation, but their adducts are less stable.[57] Since this phenomenon is observed to be time-dependent,[57] it is likely that the static 4-hour time point did not reflect the true performance of tuning the aromatic ring with various substituents. However, analysis of increasing time-points is limited by the likelihood of probe degradation in aqueous solutions, forbidding accurate time-dependent analyses of these probes. Alternatively, the substituents on the aromatic ring might abrogate the activation of the probe by β-Gal. Therefore, we conducted a molecular docking study to elucidate the binding conformation of our probes with *Escherichia coli* β-Gal to provide insights into whether these modifications produce a steric hindrance effect towards β-Gal activation.

## Molecular docking study

To elucidate the binding conformation of our probes with *Escherichia coli* β-Gal, we performed a molecular docking study within the active site (Fig. 3). To better compare the binding modes across all probes, we selected the binding conformations that adopted a similar binding mode at the β-galactoside moiety. For all probes, the β-galactoside moiety forms polar interactions with Asn102, Asp201, Glu461, and His540. Unlike the other probes, **BG-FITC-Me-1F** lacks polar interactions with His540. This can be explained by the steric hindrance at the peripheral of the binding pocket caused by the monofluoromethyl group on the self-immolative phenol linker, leading to a small torsion on the β-galactoside moiety. Notably, the catalytic residue Glu461, which serves as the proton donor in the enzyme-catalyzed hydrolysis reaction, is in proximity to the

glycosidic bond of all probes. The self-immolative phenol linker moieties of our probes do not frequently interact with the periphery of the binding pocket. However, we observed occasional π–π interactions with Trp999 with both **BG-FITC-1F** and **BG-FITC-F-1F**. Across all probes, the FITC moiety did not impart many interactions, and its' binding conformations were flexible. These observations suggest that the binding conformations of our probes are stabilized primarily by the β-galactoside moiety. Overall, the molecular docking study revealed the suitable binding conformations formed by our probes at the active site of β-Gal. Furthermore, the studies suggests that the self-immolative phenol linker ring did not affect interactions with β-Gal. Therefore, potential steric hindrance of activation by β-Gal caused by the addition of relatively small substituents on the phenol ring (*e.g.*, methyl, methoxy, and fluorine) or replacement of the fluorine leaving group for the ethyl carbamate leaving group likely does not contribute to the observed labeling results.

## Assessment of cellular performance

We further characterized the labeling efficiency of these probes in the mouse colon cancer cell lines, CT26.WT and CT26.CL25 (Fig. 4). CT26.CL25 cells, stably transfected with the β-Gal encoding *lacZ* gene, overexpress β-Gal (Fig. S5). Once the probe enters the cell, β-Gal can recognize and hydrolyze the β-galactoside moiety, triggering the generation of the electrophilic QM intermediate through self-immolation. The QM intermediate, which is linked to the reporter moiety, can then be attacked by intracellular proteins such as β-Gal itself or depart from the active site of β-Gal and react with any other available nucleophilic molecules. Consequently, trapping the reporter moiety in the cell enables improvements in the sensitivity of detecting biological activity as the probe-protein adduct is less likely to efflux from the cell (Fig. 1B). Therefore, we expect a higher fluorescence intensity in CT26.CL25 cells, which overexpress β-Gal and can thus activate the self-immobilizing probe, than CT26.WT cells post-incubation with these probes.

Both cell lines were incubated with each probe (5 μM) in serum-free RPMI 1640 medium for 4-hours at 37 °C. The resulting cells were washed once with PBS (pH 7.4) and then analyzed by fluorescence activated cell sorting (FACS) (Fig. 4A). Only **BG-FITC-1F** and **BG-FITC-F-1F** showed significant contrast between CT26.CL25 and CT26.WT cells (Fig. 4B) among all probes. Surprisingly, the overall trend observed in the SDS-PAGE analysis (Fig. 2) does not translate to cell-based assays, as the labeling efficiency can be greatly influenced by the probes' cell permeability. Generally, small molecules can penetrate biological membranes *via* passive diffusion at a rate related to their lipophilicity.[59,60] We calculated the logarithm of the partition coefficient ($c \log P$) values of each probe molecule using ChemDraw Professional version 20.0.04.1 (Table S1) and plotted the cLogP for each probe against the mean fluorescence intensities of CT26.CL25 cells after 4-hour incubation (Fig. 4C). Seemingly, there is a positive correlation between $c \log P$ and the mean fluorescence intensity of CT26.CL25 cells, suggesting that the probes' lipophilicity and resulting cell
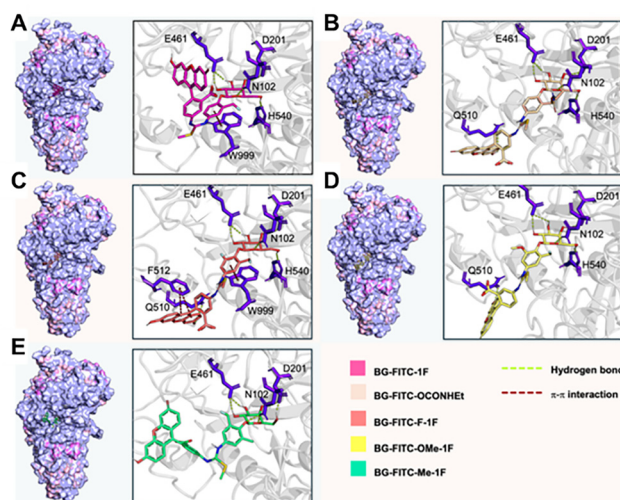


Fig. 3 The interaction map of the complex of *Escherichia coli* β-Gal (PDB: 1JYX) with (A) **BG-FITC-1F**, (B) **BG-FITC-OCONHEt**, (C) **BG-FITC-F-1F**, (D) **BG-FITC-OMe-1F**, or (E) **BG-FITC-Me-1F**. The amino acids shown have interactions with the probe molecule.
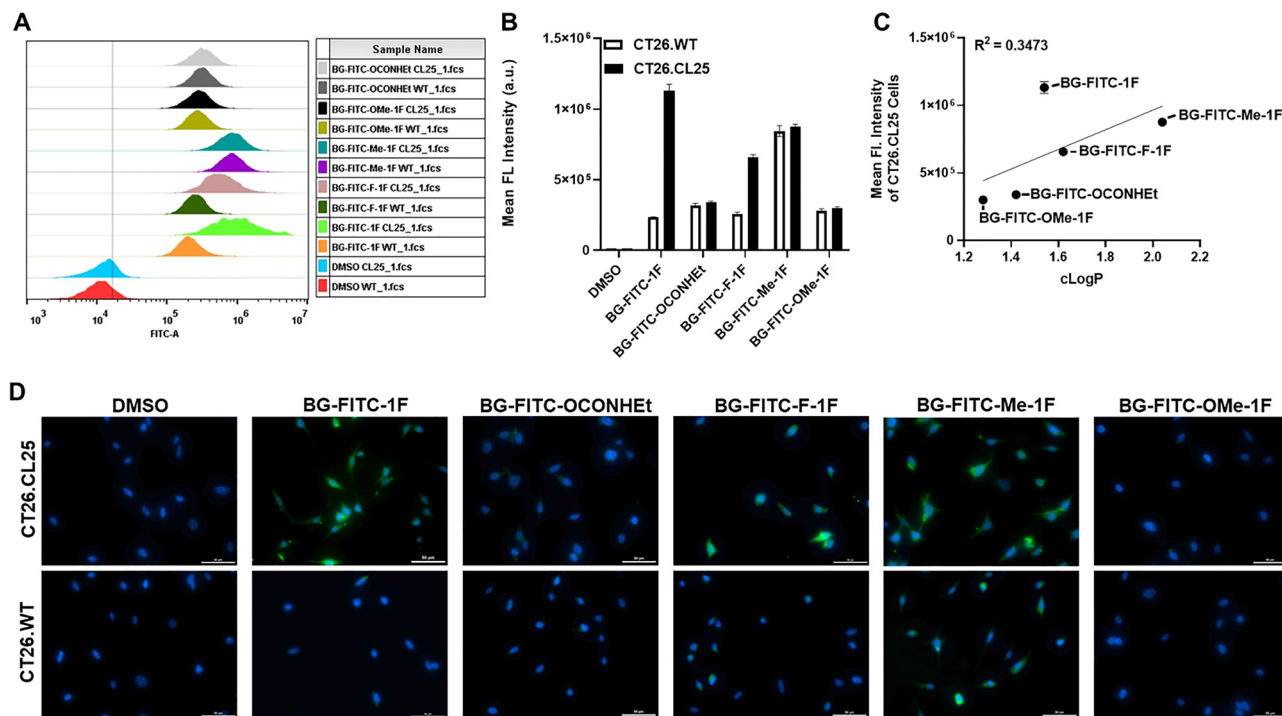
Fig. 4 Assessment of the cellular performance of **BG-FITC-1F**, **BG-FITC-OCONHEt**, **BG-FITC-F-1F**, **BG-FITC-Me-1F**, and **BG-FITC-OMe-1F** to detect β-Gal activity. (A) FACS analysis of CT26.CL25 and CT26.WT cells after incubation with probes (5 μM) or vehicle control (DMSO) for 4-hours at 37 °C. (B) Quantification of the average fluorescence intensity from (A). (C) Correlation between $c \log P$ and the average fluorescence intensity of CT26.CL25 cells after incubation with probes (5 μM) for 4-hours. The $c \log P$ values were calculated using ChemDraw Professional version 20.0.0.41. (D) Fluorescent cell imaging of CT26.CL25 and CT26.WT cells after incubation with each probe (5 μM) or vehicle control (DMSO) for 4-hours at 37 °C. Images were acquired using a Nikon Eclipse Ti2 fluorescence microscope (20× objective). Channels: DAPI (blue, $\lambda_{ex} = 375/28$ nm, $\lambda_{em} = 460/50$ nm) and FITC (green, $\lambda_{ex} = 480/30$ nm, $\lambda_{em} = 535/20$ nm). Scale bar: 50 μm. All images were acquired using the same settings.

penetration capabilities is a factor affecting these probes labeling efficiencies. Subsequently, cross-comparison of self-immobilizing probes with various degrees of lipophilicity in living cells is not straightforward, due to the possible different rates of cell penetration. Interestingly, **BG-FITC-Me-1F** was the most lipophilic of all the probes (indicated by its high $c \log P$ value), however, it exhibited high fluorescence intensities in both cell lines leading to poor contrast. SDS-PAGE analysis revealed that **BG-FITC-Me-1F** also exhibited the highest level of non-specific BSA labeling, suggesting that the poor contrast between the two cell lines is largely due to its non-specific interaction. Therefore, optimizing probe hydrophobicity is a critical factor to improve specificity and contrast.

We also performed fluorescence cell imaging of CT26.CL25 and CT26.WT cells after incubation with each probe (5 μM) in serum-free RPMI 1640 medium for 4-hours at 37 °C (Fig. 4D). Cell imaging also demonstrated a similar result as FACS analysis with only **BG-FITC-1F** and **BG-FITC-F-1F** exhibiting significant contrast, and **BG-FITC-1F** had a higher labeling efficiency than **BG-FITC-F-1F**. It is possible that **BG-FITC-F-1F** yielded less labeling efficiency than **BG-FITC-1F** because the rate of formation of QMs bearing an electron-withdrawing substituent such as fluorine is slower, resulting in inferior contrast. This phenomenon has been observed by others previously in buffered conditions.[57] Therefore, when developing

QM-based probes, we observed that the kinetics of protein adduct formation and the probes stability and lipophilicity are important parameters to be considered.

## Conclusions

While QM chemistry is highly desirable in the field of chemical biology, drug discovery, and molecular imaging, its application has been impeded by the difficulty in choosing the proper self-immolative linker to generate the QM species. The monofluoromethyl group is very appealing in many cases for its rapid labeling reaction with proteins and the formation of stable protein-probe conjugates. However, probes containing a monofluoromethyl group tend to be hydrolyzed too fast to be used in most biological applications. In this work, we tuned the self-immolative phenol linker chemistry to investigate the reactivity and stability of the QM that would allow *in situ* labeling of biological molecules with an imaging reporter *via* the generation of the QM species. For this purpose, we designed and synthesized various "always-on" fluorescent QM-based probes, each carrying a β-gal-sensitive "blocking" unit, a self-immolative phenol linker, and a FITC reporter. The self-immolative phenol linker featured either different leaving groups (*i.e.*, the widely used monofluoromethy group or ethyl

carbamate) or substituents on the phenol linker to investigate their effects on the labeling efficiency of proteins, which depends on both the stability and reactivity of the probe molecule and protein-probe conjugate. The labeling efficiency of these probes were compared in parallel through SDS-PAGE gel analysis, flow cytometry, and fluorescence cell imaging. In addition to its excellent stability in solution, in-gel fluorescence analysis suggested that the ethyl carbamate leaving group, **BG-FITC-OCONHEt**, provides higher labeling efficiency over the fluorine leaving group of the monofluoromethyl moiety, **BG-FITC-1F**. In cells, **BG-FITC-1F** had a superior labeling efficiency producing improved imaging sensitivity, likely due to better cell penetration. Therefore, from this study, we conclude that it is important to factor in the probes molecules stability, kinetics of QM formation, and cell penetration ability towards the successful application of QM-based probes. Moreover, the results from this work can be used to guide the development of QM-based probes for various other applications where FITC can be replaced by the functional moieties of choice.

## Author contributions

Z. M. R., J. L. and L. C. conceived and designed the project. Z. M. R. and J. L. performed all the chemical synthesis and compound characterization. Z. M. R., S. A., Z. C., C. C., and A. L. S. performed gel electrophoresis, fluorescence microscopy, and flow cytometry. Y. Z. performed docking study. Z. M. R., J. L., Z. C., and L. C. wrote the paper, and all authors commented on the paper.

## Conflicts of interest

There are no conflicts to declare.

## Data availability

The data supporting this article have been included as part of the supplementary information (SI). Supplementary information is available. See DOI: **https://doi.org/10.1039/d5cb00138b**.

## Acknowledgements

## Notes and references

1 R. Weissleder and U. Mahmood, Molecular Imaging, *Radiology*, 2001, **219**(2), 316–333.
2 C. Yang, Q. Wang and W. Ding, Recent progress in the imaging detection of enzyme activities *in vivo*, *RSC Adv.*, 2019, **9**(44), 25285–25302.
3 S.-D. Li and L. Huang, Pharmacokinetics and Biodistribution of Nanoparticles, *Mol. Pharmaceutics*, 2008, **5**(4), 496–504.
4 I. Johnson, Review: Fluorescent probes for living cells, *Histochem. J.*, 1998, **30**(3), 123–140.
5 K. Chen and X. Chen, Design and development of molecular imaging probes, *Curr. Top. Med. Chem.*, 2010, **10**(12), 1227–1236.
6 L. E. Edgington, M. Verdoes and M. Bogyo, Functional imaging of proteases: recent advances in the design and application of substrate-based and activity-based probes, *Curr. Opin. Chem. Biol.*, 2011, **15**(6), 798–805.
7 G.-B. Qi, Y.-J. Gao, L. Wang and H. Wang, Self-Assembled Peptide-Based Nanomaterials for Biomedical Imaging and Therapy, *Adv. Mater.*, 2018, **30**(22), 1703444.
8 Z. Hai and G. Liang, Intracellular Self-Assembly of Nanoprobes for Molecular Imaging, *Adv. Biosyst.*, 2018, **2**(8), 1800108.
9 Y. Gao, J. Shi, D. Yuan and B. Xu, Imaging enzyme-triggered self-assembly of small molecules inside live cells, *Nat. Commun.*, 2012, **3**(1), 1033.
10 G. Liang, H. Ren and J. Rao, A biocompatible condensation reaction for controlled assembly of nanostructures in living cells, *Nat. Chem.*, 2010, **2**(1), 54–60.
11 D. Ye, A. J. Shuhendler, L. Cui, L. Tong, S. S. Tee, G. Tikhomirov, D. W. Felsher and J. Rao, Bioorthogonal cyclization-mediated in situ self-assembly of small-molecule probes for imaging caspase activity in vivo, *Nat. Chem.*, 2014, **6**(6), 519–526.
12 S. Onogi, H. Shigemitsu, T. Yoshii, T. Tanida, M. Ikeda, R. Kubota and I. Hamachi, In situ real-time imaging of self-sorted supramolecular nanofibres, *Nat. Chem.*, 2016, **8**(8), 743–752.
13 J. Li, Y. Gao, Y. Kuang, J. Shi, X. Du, J. Zhou, H. Wang, Z. Yang and B. Xu, Dephosphorylation of d-Peptide Derivatives to Form Biofunctional, Supramolecular Nanofibers/Hydrogels and Their Potential Applications for Intracellular Imaging and Intratumoral Chemotherapy, *J. Am. Chem. Soc.*, 2013, **135**(26), 9907–9914.
14 Z. Chen, M. Chen, Y. Cheng, T. Kowada, J. Xie, X. Zheng and J. Rao, Exploring the Condensation Reaction between Aromatic Nitriles and Amino Thiols To Optimize In Situ Nanoparticle Formation for the Imaging of Proteases and Glycosidases in Cells, *Angew. Chem., Int. Ed.*, 2020, **59**(8), 3272–3279.
15 Z. Chen, M. Chen, K. Zhou and J. Rao, Pre-targeted Imaging of Protease Activity through In Situ Assembly of Nanoparticles, *Angew. Chem., Int. Ed.*, 2020, **59**(20), 7864–7870.
16 K. A. Schleyer, B. D. Datko, B. Burnside, C. Cui, X. Ma, J. K. Grey and L. Cui, Responsive Fluorophore Aggregation Provides Spectral Contrast for Fluorescence Lifetime Imaging, *ChemBioChem*, 2020, **21**(15), 2196–2204.
17 S. De Cesco, J. Kurian, C. Dufresne, A. K. Mittermaier and N. Moitessier, Covalent inhibitors design and discovery, *Eur. J. Med. Chem.*, 2017, **138**, 96–114.
18 L. Boike, N. J. Henning and D. K. Nomura, Advances in covalent drug discovery, *Nat. Rev. Drug Discovery*, 2022, **21**(12), 881–898.

19 G. Blum, G. von Degenfeld, M. J. Merchant, H. M. Blau and M. Bogyo, Noninvasive optical imaging of cysteine protease activity using fluorescently quenched activity-based probes, *Nat. Chem. Biol.*, 2007, **3**(10), 668–677.

20 G. Blum, S. R. Mullins, K. Keren, M. Fonovič, C. Jedeszko, M. J. Rice, B. F. Sloane and M. Bogyo, Dynamic imaging of protease activity with fluorescently quenched activity-based probes, *Nat. Chem. Biol.*, 2005, **1**(4), 203–209.

21 L. E. Edgington, A. B. Berger, G. Blum, V. E. Albrow, M. G. Paulick, N. Lineberry and M. Bogyo, Noninvasive optical imaging of apoptosis by caspase-targeted activity-based probes, *Nat. Med.*, 2009, **15**(8), 967–973.

22 D. H. Kwan, H.-M. Chen, K. Ratananikom, S. M. Hancock, Y. Watanabe, P. T. Kongsaeree, A. L. Samuels and S. G. Withers, Self-Immobilizing Fluorogenic Imaging Agents of Enzyme Activity, *Angew. Chem., Int. Ed.*, 2011, **50**(1), 300–303.

23 W.-J. Bai, J. G. David, Z.-G. Feng, M. G. Weaver, K.-L. Wu and T. R. R. Pettus, The Domestication of ortho-Quinone Methides, *Acc. Chem. Res.*, 2014, **47**(12), 3655–3664.

24 M. S. Singh, A. Nagaraju, N. Anand and S. Chowdhury, ortho-Quinone methide (o-QM): a highly reactive, ephemeral and versatile intermediate in organic synthesis, *RSC Adv.*, 2014, **4**(99), 55924–55959.

25 A. Minard, D. Liano, X. Wang and M. Di Antonio, The unexplored potential of quinone methides in chemical biology, *Bioorg. Med. Chem.*, 2019, **27**(12), 2298–2305.

26 D. Kern and A. Kormos, Self-Immobilizing Quinone Methides for the Fluorescent Sensing of Enzyme Activity, *Chemosensors*, 2023, **11**, 3.

27 A. Abe and M. Kamiya, A versatile toolbox for investigating biological processes based on quinone methide chemistry: From self-immolative linkers to self-immobilizing agents, *Bioorg. Med. Chem.*, 2021, 44.

28 J. R. Betley, S. Cesaro-Tadic, A. Mekhalfia, J. H. Rickard, H. Denham, L. J. Partridge, A. Plückthun and G. M. Blackburn, Direct Screening for Phosphatase Activity by Turnover-Based Capture of Protein Catalysts, *Angew. Chem., Int. Ed.*, 2002, **41**(5), 775–777.

29 M. Kurogochi, S.-I. Nishimura and Y. C. Lee, Mechanism-based fluorescent labeling of β-galactosidases. An efficient method in proteomics for glycoside hydrolases, *J. Biol. Chem.*, 2004, **279**, 44704–44712.

30 T.-C. Cheng, S. R. Roffler, S.-C. Tzou, K.-H. Chuang, Y.-C. Su, C.-H. Chuang, C.-H. Kao, C.-S. Chen, I. H. Harn, K.-Y. Liu, T.-L. Cheng and Y.-L. Leu, An Activity-Based Near-Infrared Glucuronide Trapping Probe for Imaging β-Glucuronidase Expression in Deep Tissues, *J. Am. Chem. Soc.*, 2012, **134**(6), 3103–3110.

31 Y.-L. Hsu, M. Nandakumar, H.-Y. Lai, T.-C. Chou, C.-Y. Chu, C.-H. Lin and L.-C. Lo, Development of Activity-Based Probes for Imaging Human α-l-Fucosidases in Cells, *J. Org. Chem.*, 2015, **80**(16), 8458–8463.

32 L. M. Chauvigné-Hines, L. N. Anderson, H. M. Weaver, J. N. Brown, P. K. Koech, C. D. Nicora, B. A. Hofstad, R. D. Smith, M. J. Wilkins, S. J. Callister and A. T. Wright, Suite of Activity-Based Probes for Cellulose-Degrading Enzymes, *J. Am. Chem. Soc.*, 2012, **134**(50), 20521–20532.

33 C.-P. Lu, C.-T. Ren, Y.-N. Lai, S.-H. Wu, W.-M. Wang, J.-Y. Chen and L.-C. Lo, Design of a Mechanism-Based Probe for Neuraminidase To Capture Influenza Viruses, *Angew. Chem., Int. Ed.*, 2005, **44**(42), 6888–6892.

34 M. A. Lumba, L. M. Willis, S. Santra, R. Rana, L. Schito, S. Rey, B. G. Wouters, M. Nitz and A. β-galactosidase, probe for the detection of cellular senescence by mass cytometry, *Org. Biomol. Chem.*, 2017, **15**(30), 6388–6392.

35 C.-S. Tsai, Y.-K. Li and L.-C. Lo, Design and Synthesis of Activity Probes for Glycosidases, *Org. Lett.*, 2002, **4**(21), 3607–3610.

36 J. Jiang, Q. Tan, S. Zhao, H. Song, L. Hu and H. Xie, Late-stage difluoromethylation leading to a self-immobilizing fluorogenic probe for the visualization of enzyme activities in live cells, *Chem. Commun.*, 2019, **55**(99), 15000–15003.

37 Z. Gao, A. J. Thompson, J. C. Paulson and S. G. Withers, Proximity Ligation-Based Fluorogenic Imaging Agents for Neuraminidases, *Angew. Chem., Int. Ed.*, 2018, **57**(41), 13538–13541.

38 J. Liu, X. Ma, C. Cui, Z. Chen, Y. Wang, P. R. Deenik, L. Cui and N. I. R. Noninvasive, Imaging of Senescence via In Situ Labeling, *J. Med. Chem.*, 2021, **64**(24), 17969–17978.

39 Y.-Y. Huang, C.-C. Kuo, C.-Y. Chu, Y.-H. Huang, Y.-L. Hu, J.-J. Lin and L.-C. Lo, Development of activity-based probes with tunable specificity for protein tyrosine phosphatase subfamilies, *Tetrahedron*, 2010, **66**(25), 4521–4529.

40 C. H. Tai, C. P. Lu, S. H. Wu and L. C. Lo, Synthesis and evaluation of turn-on fluorescent probes for imaging steroid sulfatase activities in cells, *Chem. Commun.*, 2014, **50**(46), 6116–6119.

41 W. Mao, L. Xia, Y. Wang, H. Xie and A. Self-Immobilizing, and Fluorogenic Probe for β-Lactamase Detection, *Chem. – Asian J.*, 2016, **11**(24), 3493–3497.

42 T. Doura, M. Kamiya, F. Obata, Y. Yamaguchi, T. Y. Hiyama, T. Matsuda, A. Fukamizu, M. Noda, M. Miura and Y. Urano, Detection of LacZ-Positive Cells in Living Tissue with Single-Cell Resolution, *Angew. Chem., Int. Ed.*, 2016, **55**(33), 9620–9624.

43 H. Ito, Y. Kawamata, M. Kamiya, K. Tsuda-Sakurai, S. Tanaka, T. Ueno, T. Komatsu, K. Hanaoka, S. Okabe, M. Miura and Y. Urano, Red-Shifted Fluorogenic Substrate for Detection of lacZ-Positive Cells in Living Tissue with Single-Cell Resolution, *Angew. Chem., Int. Ed.*, 2018, **57**(48), 15702–15706.

44 M. Chiba, M. Kamiya, K. Tsuda-Sakurai, Y. Fujisawa, H. Kosakamoto, R. Kojima, M. Miura and Y. Urano, Activatable Photosensitizer for Targeted Ablation of lacZ-Positive Cells with Single-Cell Resolution, *ACS Cent. Sci.*, 2019, **5**(10), 1676–1681.

45 J. K. Myers and T. S. Widlanski, Mechanism-Based Inactivation of Prostatic Acid Phosphatase, *Science*, 1993, **262**(5138), 1451–1453.

46 K. Haba, M. Popkov, M. Shamis, R. A. Lerner, C. F. Barbas III and D. Shabat, Single-Triggered Trimeric Prodrugs, *Angew. Chem., Int. Ed.*, 2005, **44**(5), 716–720.

47 S. Gnaim and D. Shabat, Quinone-Methide Species, A Gateway to Functional Molecular Systems: From Self-Immolative Dendrimers to Long-Wavelength Fluorescent Dyes, *Acc. Chem. Res.*, 2014, **47**(10), 2970–2984.

48 K. D. Janda, L.-C. Lo, C.-H. L. Lo, M.-M. Sim, R. Wang, C.-H. Wong and R. A. Lerner, Chemical Selection for Catalysis in Combinatorial Antibody Libraries, *Science*, 1997, **275**(5302), 945–948.

49 S. Cesaro-Tadic, D. Lagos, A. Honegger, J. H. Rickard, L. J. Partridge, G. M. Blackburn and A. Plückthun, Turnover-based in vitro selection and evolution of biocatalysts from a fully synthetic antibody library, *Nat. Biotechnol.*, 2003, **21**(6), 679–685.

50 J. Liu, L. Cai, W. Sun, R. Cheng, N. Wang, L. Jin, S. Rozovsky, I. B. Seiple and L. Wang, Photocaged Quinone Methide Crosslinkers for Light-Controlled Chemical Crosslinking of Protein–Protein and Protein–DNA Complexes, *Angew. Chem., Int. Ed.*, 2019, **58**(52), 18839–18843.

51 J. Y. Hyun, S.-H. Park, C. W. Park, H. B. Kim, J. W. Cho and I. Shin, Trifunctional Fluorogenic Probes for Fluorescence Imaging and Isolation of Glycosidases in Cells, *Org. Lett.*, 2019, **21**(12), 4439–4442.

52 Y. Li, H. Song, C. Xue, Z. Fang, L. Xiong and H. Xie, A self-immobilizing near-infrared fluorogenic probe for sensitive imaging of extracellular enzyme activity in vivo, *Chem. Sci.*, 2020, **11**(23), 5889–5894.

53 H. Song, Y. Li, Y. Chen, C. Xue and H. Xie, Highly Efficient Multiple-Labeling Probes for the Visualization of Enzyme Activities, *Chem. – Eur. J.*, 2019, **25**(61), 13994–14002.

54 V. Ahmed, Y. Liu and S. D. Taylor, Multiple Pathways for the Irreversible Inhibition of Steroid Sulfatase with Quinone Methide-Generating Suicide Inhibitors, *ChemBioChem*, 2009, **10**(9), 1457–1461.

55 Y. Miao, Z. Q. Yu, S. Xu and M. Yan, Quinone Methide Based Self-Immobilizing Molecular Fluorescent Probes for In Situ Imaging of Enzymes, *Chem. Asian J.*, 2024, **19**, e202400189.

56 Y. Li, C. Xue, Z. Fang, W. Xu and H. Xie, In Vivo Visualization of γ-Glutamyl Transpeptidase Activity with an Activatable Self-Immobilizing Near-Infrared Probe, *Anal. Chem.*, 2020, **92**(22), 15017–15024.

57 E. E. Weinert, R. Dondi, S. Colloredo-Melz, K. N. Frankenfield, C. H. Mitchell, M. Freccero and S. E. Rokita, Substituents on quinone methides strongly modulate formation and stability of their nucleophilic adducts, *J. Am. Chem. Soc.*, 2006, **128**(36), 11940–11947.

58 E. E. Weinert, K. N. Frankenfield and S. E. Rokita, Time-dependent evolution of adducts formed between deoxynucleosides and a model quinone methide, *Chem. Res. Toxicol.*, 2005, **18**(9), 1364–1370.

59 P. D. Dobson and D. B. Kell, Carrier-mediated cellular uptake of pharmaceutical drugs: an exception or the rule?, *Nat. Rev. Drug Discovery*, 2008, **7**(3), 205–220.

60 A. K. Ghose, V. N. Viswanadhan and J. J. Wendoloski, Prediction of Hydrophobic (Lipophilic) Properties of Small Organic Molecules Using Fragmental Methods: An Analysis of ALOGP and CLOGP Methods, *J. Phys. Chem. A*, 1998, **102**(21), 3762–3772.